ISBN: 978-3-95450-214-1 ISSN: 2673-5490 doi:10.18429/JACoW-IPAC2021-WEPAB210

BEAM COMMISSIONING OF THE NEW 160 MeV H⁻ INJECTION SYSTEM OF THE CERN PS BOOSTER

E. Renner*[1], S. Albright, F. Antoniou, F. Asvesta, H. Bartosik, C. Bracco, G. P. Di Giovanni, L. Jorat, E. H. Maclean, M. Meddahi, B. Mikulec, G. Rumolo, T. Prebibaj, P. Skowronski, W. Weterings, CERN, Geneva, Switzerland
[1]also at TU Wien, Vienna, Austria

Abstract

A key component to meeting the brightness targets of the LHC Injectors Upgrade (LIU) project at CERN is the new 160 MeV H⁻ charge exchange injection system into the Proton Synchrotron Booster. This system has been in beam commissioning since December 2020, optimizing the beam production schemes for tailoring different beams to the respective user-defined brightness targets. In this paper, selected measurements from the beam commissioning period are presented, characterizing the system's flexibility to produce the required wide range of transverse emittances. The discussion focuses on the essential optimization of the injection set-up to minimize space charge driven emittance blow-up and injection errors. The results are completed by selected comparisons with multi-particle simulation models of the injection process.

INTRODUCTION

The CERN Proton Synchrotron Booster (PSB) is the first synchrotron in the CERN injector complex and is used for tailoring the wide range of transverse beam characteristics as requested by the various users at CERN, covering intensities from $N_{p_+} = \mathcal{O}(10^{10})$ to $\mathcal{O}(10^{13})$ protons and normalized transverse emittances from $\epsilon_{n,\mathrm{rms}}$ <0.7 µm (LHC-like beams) to ≈ 9−10 µm (high intensity beams). As part of the LHC Injectors Upgrade (LIU) [1] project, the PSB was upgraded during the Long Shut Down 2 (LS2) in 2019/2020. A major aspect of this upgrade was the connection of the newly built Linac4 [2] to the PSB, increasing the injection energy from 50 to 160 MeV and hence the relativistic factor $\beta_r\gamma_r^2$ by a factor of two. This increased injection energy allows the beam brightness to be doubled, as required for the High Luminosity era of LHC (HL-LHC), while maintaining the tune-spread induced by space charge as pre-LS2: $\Delta Q \propto N_{p_+}/(\gamma_r^2\beta_r) \approx -0.5$.

To inject the 160 MeV H⁻ beam, a new charge exchange injection system has been installed, replacing a conventional proton multi-turn injection. In addition to providing the required HL-LHC beam brightness, this scheme results inherently in a significant reduction of the injection losses, which is particularly relevant for high intensity beams. Horizontal phase space painting further enables direct tailoring and optimization of the targeted phase space distributions.

Commissioning of the upgraded PS Booster was started in December 2020 and is currently ongoing. In this paper, first beam profile measurements, performed with wire scanners, are presented in order to probe both the new system's sensitivity to injection imprecision, relevant for users requiring $\epsilon_{u,\mathrm{rms}} \lesssim 1$ µm, as well as the application of phase space painting for tailoring high intensity beams.

SYSTEM LAYOUT

The H⁻ beam coming from Linac4 features normalized transverse emittances $\epsilon_{u,n} \approx 0.3$ µm in both planes $u = x, y$ and can be accumulated over 150 turns in the PSB, which has a revolution period $\tau \approx 1$ µs at 160 MeV.

The new system (Fig. 1) [3] comprises a carbon stripping foil of ≈200 µg cm^{-2} density, a chicane in the injection region (BSW) [4] and painting kicker magnets (KSW) [5]. Figure 2 illustrates the programmable painting bump field decay, which enables customizing the horizontal phase space painting for each user. The vertical beam size can be tailored by applying a fixed vertical offset Δy to the injected beam.

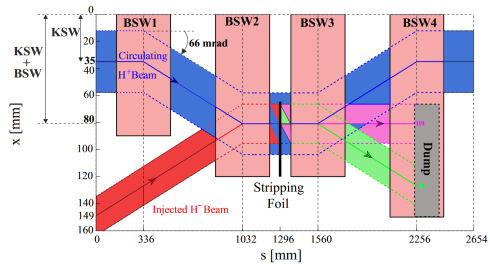

Figure 1: Schematic of the PSB H⁻ injection system [1].

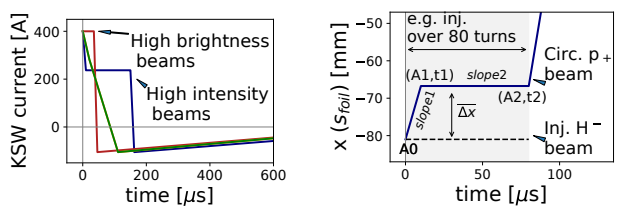

(a) KSW decay for different users. (b) Beam position at the foil.

Figure 2: Schematics of the painting bump (KSW).

BEAM MEASUREMENTS

The parameters for the here presented beam tests are summarized in Table 1. All presented wire-scans are taken at extraction energy at the end of the cycle. Comparative multi-particle simulations of the injection process, done with PTC-pyOrbit [6], are conducted for the first 5 ms. Approximate ranges for the expected extent of the space charge tune spread

* elisabeth.renner@cern.ch

ISBN: 978-3-95450-214-1 ISSN: 2673-5490 doi:10.18429/JACoW-IPAC2021-WEPAB210

Table 1: Settings for the Presented Measurements (dE_{rms}: r.m.s. Energy Spread of the Injected Longitudinal Distribution; Q_x/Q_y: Working Point at Injection (t_i) and Extraction (t_e); $\Delta Q_{x,\mathrm{max}}/\Delta Q_{y,\mathrm{max}}$: Expected Maximum Tune Spread at Injection)

Measurement	Int. [p+]	dE_{rms}	$Q_x/Q_y : t_i$	$Q_x/Q_y : t_e$	$\lvert Q_{x,\mathrm{max}}\rvert$	$\lvert Q_{y,\mathrm{max}}\rvert$
Foil scattering	$1.5{\cdot}10^{11}$	100 keV	4.17/4.23	4.17/4.23	for $N_t \gtrsim 50$: $\lesssim 0.15$, else $\gtrsim 0.15$	$N_t \gtrsim 50$: $\lesssim 0.2$, else $\gtrsim 0.2$
Injection error	$1.0{\cdot}10^{11}$	440 keV	4.17/4.23	4.17/4.23	$\lesssim 0.1$	$\lesssim 0.1$
Phase space painting	$8 \cdot 10^{12}$	440 keV	4.22/4.41	4.17/4.23	for $\overline{\Delta x} \gtrsim 10$ mm: $\lesssim 0.25$, else $\gtrsim 0.25$	$\lesssim 0.4$

Table 2: Characteristics of the Measured Stripping Foils

Type	Thickness	Description
1 / XCF-200	200 µg cm^{-2}	Arc evaporated amorphous Carbon [7]
2 / MLG-250	240 µg cm^{-2}	Multilayer Graphene [8]
3 / GSI-200	200 µg cm^{-2}	Arc evaporated amorphous Carbon [9]

are given in Table 1. When comparing the simulation results to the measured distributions, the simulated profiles are scaled with the beam energy. Based on the chosen working points, no significant emittance degradation is expected between injection and extraction. The profile measured at extraction energy is thus expected to reflect the variation due to the different injection settings in first approximation.

Characterization of Foil Scattering Induced Emittance Increase

The characteristics of the 200 µg cm^{-2} carbon stripping foil are selected in order to provide sufficient stripping efficiency (>99 %), while minimizing the emittance blowup, and hence the degradation of the beam brightness, induced by foil scattering [10]. In 2018/2019 foils of different manufactures have been qualified regarding stripping efficiency and lifetime in a test stand installed in the Linac4 transfer line [11,12]. However, due to the single foil passage, a verification of the predicted scattering properties was not possible. Now, in the PSB, the flexibility to customize the number of foil crossings enables an assessment of the emittance increase induced by multiple passages through the foils.

Generally, for an r.m.s. scattering angle of a multi-Coulomb scattered distribution $\sqrt{\langle\Theta^2\rangle}$, the expected emittance increase $\Delta\epsilon_{u,\mathrm{rms}}$ can be approximated by

$$\Delta\epsilon_{u,\mathrm{rms,foil}} = 0.5 \cdot \beta_u \langle\Theta^2\rangle \qquad (1)$$

and is hence proportional to the beta function β_u. The average scattering angle can be analytically approximated using Moliere's formula (Eq. (2)) with the logarithmic correction for thin targets [13–15]:

$$\sqrt{\langle\Theta^2\rangle} = \frac{13.6}{p[\mathrm{MeV/c}]\beta_r}\sqrt{\frac{N_t \cdot d}{L_{\mathrm{rad}}}}\cdot\left(1 + 0.038 \cdot \ln\frac{N_t \cdot d}{L_{\mathrm{rad}}}\right) \qquad (2)$$

with $L_{\mathrm{rad}} = 19$ cm as the carbon radiation length, the speed of light c, the beam momentum p, the relativistic factor β_r, the number of foil crossings N_t and the equivalent foil thickness $d = 0.9$ µm, derived from the given foil thickness of 200 µg cm^{-2}. In the multi-particle simulations, foil scattering is considered assuming a repeated single Coulomb scattering model [16], which approaches a distribution as obtained with Eq. (1) for multiple foil passages.

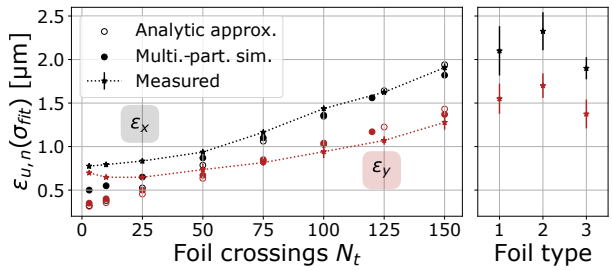

Figure 3: Left: Transverse emittances for varying number of foil hits N_t, foil type 3. Right: Different foil types, $N_t = 150$.

Figure 3 illustrates $\epsilon_{u,\mathrm{rms}}$, measured for a varying number of foil crossings of the GSI-200 foil (type 3, see Table 2). Analytical and simulation results show an agreement with the measurements for $N_t >$ 30-50. Considering the in Table 1 listed beam parameters, samples with $N_t < 30-50$ feature an increased tune spread during the first ms, explaining the observed increased emittance due to interaction with resonances. Beta-beating in the machine can cause a discrepancy between measurements and simulations due to a change of optics at the foil compared to the theoretically considered $\beta_x = 5.7$ m and $\beta_y = 4$ m. Figure 3 (right) further summarizes the measurements for $N_t = 150$ obtained in ring 2 and 3 for the different foil types as listed in Table 2. For all tested foils, the measured $\Delta\epsilon_{u,\mathrm{rms,foil}}$ is consistent with the model. No significant foil induced beam degradation is expected for any foil type for the production of high brightness beams (10 to 35 injected turns).

Sensitivity to Injection Errors

An additional aspect for providing the requested beam brightness for LHC beams is the minimization of injection imperfections due to steering errors and field ripples. The impact of optics mismatch plays a less pronounced role and is hence not taken into account in this report. The increase of the $\epsilon_{u,\mathrm{rms}}$ by steering errors in position Δu and angle $\Delta u'$, can be written as

$$\frac{\epsilon_{u,\mathrm{rms}}}{\epsilon_{u,\mathrm{rms},0}} = 1 + \frac{1}{2}\frac{\Delta u^2 + (\beta_u\Delta u' + \alpha_u\Delta u)^2}{\beta_u\epsilon_{u,\mathrm{rms},0}}, \qquad (3)$$

considering the Twiss parameters β_u and α_u. Based on analytic considerations and complementary simulations, an injection precision of $\Delta u_{max} \lesssim 1.5 - 2.0$ mm, assuming $\Delta u' = 0$ mrad is required to produce beams within the target $\epsilon_{u,\mathrm{rms},n} \lesssim 0.6 - 0.7$ µm. Currently, when injecting a single turn, injection oscillations are minimized to a level of ±0.5 mm in both planes. Still, shot to shot fluctuations, depending on the super-cycle composition can occur. When injecting multiple turns reproducible transverse fluctuations

ISBN: 978-3-95450-214-1 ISSN: 2673-5490 doi:10.18429/JACoW-IPAC2021-WEPAB210

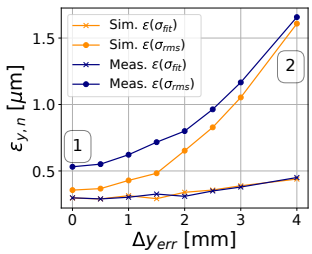

(a) $\epsilon_{y,n}$ for different vert. offsets.

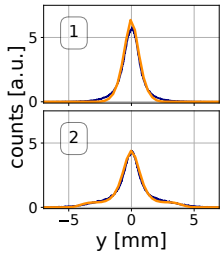

(b) Vert. profiles.

Figure 4: Sensitivity study to vertical injection errors.

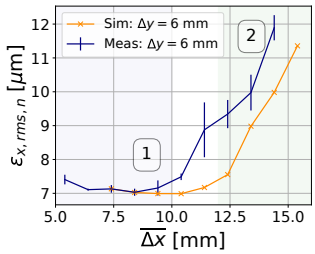

(a) $\epsilon_{x,\mathrm{rms},n}$ for diff. painting schemes.

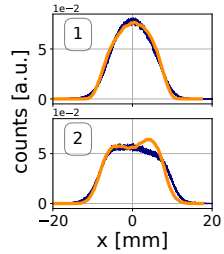

(b) Horiz. profiles.

Figure 5: Painting studies for high intensity beams.

of up to $\pm$ 1 − 2 mm inside the beam pulse can be present due to field ripples of transfer-line elements and variation along the Linac4 pulse.

The evolution of $\epsilon_{y,n}$ has been measured to benchmark the dependence on vertical offsets Δy (Fig. 4a). It has to be emphasized that injection errors cause population of the transverse tails during filamentation while not causing a significant increase in the Gaussian fit of the core. Whereas Eq. (3) describes the increase in the r.m.s emittance, it gives no information about the tail population. The results are thus presented by comparing both, the $\epsilon_{y,n}$ calculated from the r.m.s. beam size σ_{rms} (circles) as well as σ_{fit} obtained when fitting a Gaussian distribution (crosses).

The results show a good agreement between simulations and measurements for $\epsilon(\sigma_{\mathrm{fit}})$. However, an increased tail population and hence and increased ratio $\epsilon_{y,n}(\sigma_{\mathrm{rms}})/\epsilon_{y,n}(\sigma_{\mathrm{fit}})$ is observed in measurements compared to simulations for small Δy. The generation of these tails is still under investigation. Studies are ongoing to disentangle the contributions originating from the injected beam distribution, distortions from the wire scanner measurements [17] and evolution of these tails during the PSB cycle. Still, a general trend of beam profile degradation when increasing the applied Δy is confirmed.

Phase Space Painting for High Intensity Beams

Painting schemes to tailor the emittances for the various fixed target beams and minimize losses while pushing the injected intensity to $I > 1.1 \cdot 10^{13}$ p+ have been defined in simulations prior to the PSB restart [18–20]. Verification, adaptation and (online) optimization studies of the proposed painting schemes are ongoing in order to exploit the new system's painting flexibility. Generally, for high intensity beams, the baseline approach is to apply a fast initial painting bump decay (slope 1, Fig. 2) within the first 8-15 µs (turns) in order to reduce the charge density in the beam core and hence the space charge tune spread ΔQ_x. A subsequent plateau (slope 2) with slow offset variation is used to accumulate the target intensity over a defined number of injected turns.

First proof-of-principle results of phase space painting using beams for the ISOLDE experimental facility with pre-LS2 intensities ($\approx 8 \cdot 10^{12}$ p+ per PSB ring, beam accumulation over 80 turns) are compared to multi-particle simulations in Fig. 5a. The average offset between the injected and circulating beam, $\overline{\Delta x} = A0 - (A1 + A2)/2$, is varied and the response of the measured $\epsilon_{x,\mathrm{rms},n}$ assessed, while keeping the applied Δy constant (5 and 6 mm). For this intensity, the increased charge density for small $\overline{\Delta x}$ (i.e. $\lessapprox$10 mm) causes $|\Delta Q_x| \gtrsim 0.2$. The consequent interaction of the beam with the horizontal resonances at integer tunes defines the resulting $\epsilon_{x,\mathrm{rms},n}$ (blue-shaded in Fig. 5a). Instead, $\overline{\Delta x} \gtrsim 10$ mm reduces $|\Delta Q_x| \lessapprox 0.2$ and the emittance increase is dominated by the applied painting (green-shaded). The characteristics of this transition from controlled emittance tailoring, profiting from the phase space painting, to a blow-up due to resonance crossing is observed similarly in simulations and measurements (respectively orange and blue in Fig. 5b).

The scope of this study is to show that with the new system phase space painting can be applied as foreseen to tailor high intensity beams. It is worth highlighting, that the achieved losses are already now within a few percent, which is a significant improvement compared to the conventional multi-turn injection pre-LS2, with 30-40% losses at the injection septum. The observed differences between the presented preliminary measurements and simulations. Further systematic studies, also taking into consideration the profile distortion induced by the wire scanner and evolution of the particle distribution along the cycle, are being performed to benchmark the models, optimize the proposed painting functions and further reduce losses.

SUMMARY

The new H^- charge exchange injection system of the PSB is currently being commissioned. Profiting of the new system's flexibility for horizontal phase space painting, first emittance tailoring studies for high intensity beams are shown to be in line with simulation results. Measurements to verify the system's response to steering errors and foil scattering are presented. General agreement with simulation results confirms the specified margins for injection errors as well as the suitability of the installed stripping foils regarding emittance degradation due to foil scattering. The performance reached with the new PSB H^- injection is already now approaching the brightness goals for the production of the HL-LHC beam.

ACKNOWLEDGMENTS

The authors would like to thank all teams involved in the PSB and Linac4 operation, hardware and beam commissioning for their continuous support and input.

ISBN: 978-3-95450-214-1 ISSN: 2673-5490 doi:10.18429/JACoW-IPAC2021-WEPAB210

REFERENCES

[1] J. Coupard *et al.*, "LHC Injectors Upgrade, Technical Design Report, Vol. I: Protons", CERN, Geneva, Switzerland, Rep. CERN-ACC-2014-0337. 2014.

[2] L. Arnaudon *et al.*, "Linac4 Technical Design Report", CERN, Geneva, Switzerland, Rep. CERN-AB-2006-084, 2006.

[3] W. J. M. Weterings, C. Bracco, L. O. Jorat, M. Meddahi, R. Noulibos, and P. Van Trappen, "The New Injection Region of the CERN PS Booster", in *Proc. 10th Int. Particle Accelerator Conf. (IPAC'19)*, Melbourne, Australia, May 2019, pp. 2414–2417. doi:10.18429/JACoW-IPAC2019-WEPMP039

[4] B. Balhan, C. Baud, C. C. M. Borburgh, and M. Hourican, "Design and Construction of the CERN PS Booster Charge Exchange Injection Chicane Bumpers", in *Proc. 9th Int. Particle Accelerator Conf. (IPAC'18)*, Vancouver, Canada, Apr.-May 2018, pp. 2575–2577. doi:10.18429/JACoW-IPAC2018-WEPMF082

[5] L. M. C. Feliciano *et al.*, "A New Hardware Design for PSB Kicker Magnets (KSW) for the 35 mm Transverse Painting in the Horizontal Plane", in *Proc. 6th Int. Particle Accelerator Conf. (IPAC'15)*, Richmond, VA, USA, May 2015, pp. 3890–3892. doi:10.18429/JACoW-IPAC2015-THPF086

[6] A. Shishlo *et al.*, "The Particle Accelerator Simulation Code PyORBIT", in *Proc. Int. Conf. on Computational Science*, Reykjavík, Iceland, Jun. 2015, pp. 1272–1281.

[7] ACF-Metals, 2239 E. Kleindale Road, Tucson, Arizona, U.S.A.

[8] Kaneka Coorperation, Nakanoshima, Kita-ku, Osaka, 530-8288

[9] GSI Helmholtzzentrum für Schwerionenforschung GmbH, Planckstraße 1, 64291 Darmstadt

[10] B. Goddard, M. Aiba, C. Bracco, C. Carli, M. Meddahi, and W. J. M. Weterings, "Stripping Foil Issues for H- Injection into the CERN PSB at 160 MeV", in *Proc. 1st Int. Particle Accelerator Conf. (IPAC'10)*, Kyoto, Japan, May 2010, paper THPEB030, pp. 3951–3953.

[11] C. Bracco *et al.*, "Commissioning of the Stripping Foil Units for the Upgrade of the PSB H- Injection System", in *Proc. 8th Int. Particle Accelerator Conf. (IPAC'17)*, Copenhagen, Denmark, May 2017, pp. 595–598. doi:10.18429/JACoW-IPAC2017-MOPIK041

[12] C. Bracco *et al.*, "Measurements with the stripping foil test stand in the Linac4 Transfer Line", in *29th World Conf. of the Int. Nuclear Target Development Society*, East Lansing, United States, Oct. 2018, p. 01003. doi:10.1051/epjconf/202022901003

[13] J.-B. Moliere, "Theorie der Streuung schneller geladener Teilchen I. Einzelstreuung am abgeschirmten Coulomb Feld", *Z. Naturforsch. A*, vol. 2, pp. 133-145, 1947. doi:10.1515/zna-1947-0302

[14] V. L. Highland, "Some Practical Remarks on Multiple Scattering", *Nuclear Instruments and Methods*, vol. 129, pp. 497-499, 1975. doi:10.1016/0029-554X(75)90743-0

[15] J. D. Jackson, *Classical Electrodynamics*, New York, NY, USA: Wiley, 1975.

[16] F. W. Jones, "User's Guide to ACCSIM", TRIUMF, Vancouver, Canada, Rep. TRIUMF TRI-DN-90-17 v.3.0, Jun. 1990.

[17] A. Santamaría García *et al.*, "Systematic Studies of Transverse Emittance Measurements Along the CERN PS Booster Cycle", in *Proc. 9th Int. Particle Accelerator Conf. (IPAC'18)*, Vancouver, Canada, Apr.-May 2018, pp. 806–809. doi:10.18429/JACoW-IPAC2018-TUPAF047

[18] V. Forte, "Performance of the CERN PSB at 160 MeV with H^- charge exchange injection", CERN, Geneva, Switzerland, Rep. CERN-THESIS-2016-063, Jun. 2016.

[19] V. Forte, C. Bracco, G. P. Di Giovanni, M. A. Fraser, A. M. Lombardi, and B. Mikulec, "Multi-Particle Simulations of the Future CERN PSB Injection Process with Updated Linac4 Beam Performance", in *Proc. 61st ICFA Advanced Beam Dynamics Workshop on High-Intensity and High-Brightness Hadron Beams (HB'18)*, Daejeon, Korea, Jun. 2018, pp. 278–283. doi:10.18429/JACoW-HB2018-WEP2PO007

[20] E. Renner *et al.*, "PSB simulation studies for post LS2 operation", presented at the 4th ICFA Mini-Workshop on Space Charge, CERN, Geneva, Switzerland, Nov. 2019, unpublished.